

A HELIUM SPREAD AMONG THE MAIN-SEQUENCE STARS IN NGC 2808

F. D'ANTONA,¹ M. BELLAZZINI,² V. CALOI,³ F. FUSI PECCI,² S. GALLETI,² AND R. T. ROOD⁴

Received 2005 April 15; accepted 2005 May 15

ABSTRACT

We have made a detailed study of the color distribution of the main sequence of the globular cluster (GC) NGC 2808, based on new deep *HST* WFPC2 photometry of a field in the uncrowded outskirts of the cluster. The observed color distribution of main-sequence stars is not Gaussian and is wider than expected for a single stellar population, given our (carefully determined) measurement errors. About 20% of the sample stars are much bluer than expected and are most plausibly explained as a population having a much larger helium abundance than the bulk of the main sequence. Using synthetic color-magnitude diagrams based on new stellar models, we estimate that the helium mass fraction of these stars is $Y \sim 0.4$. The newly found anomaly on the main sequence gives credence to the idea that GCs like NGC 2808 have undergone self-enrichment and that different stellar populations were born from the ejecta of the intermediate-mass asymptotic giant branch (AGB) stars of the first generation. The enhancement and spread of helium among the stars in NGC 2808 have recently been suggested as a simple way to explain the very peculiar morphology of its horizontal branch. We find that if in addition to the $Y = 0.40$ stars, roughly 30% of the stars have Y distributed between 0.26–0.29, while 50% have primordial Y , this leads to a horizontal-branch morphology similar to that observed. In this framework, three main stages of star formation are identified, the first with primordial helium content $Y \simeq 0.24$, the second born from the winds of the most massive AGBs of the first stellar generation ($\sim 6\text{--}7 M_{\odot}$), with $Y \sim 0.4$, and a third born from the matter ejected from less massive AGBs ($\sim 3.5\text{--}4.5 M_{\odot}$), with $Y \sim 0.26\text{--}0.29$. There could have been a long hiatus (several times 10^7 yr), between the second and third generation in which no star formed in the protocluster. We suggest that during this period, star formation has been inhibited by the explosion of late Type II supernovae deriving from binary evolution.

Subject headings: globular clusters: general — globular clusters: individual (NGC 2808)

Online material: color figures

1. INTRODUCTION

Chemical inhomogeneities in globular cluster (GC) stars supply new evidence on the formation and evolution of these most ancient stellar systems. Self-enrichment mechanisms are being examined as some of the possible—and most plausible—causes of the abundance spreads seen in many GCs. In these clusters light elements that are susceptible to abundance changes from proton-capture reactions, such as the *pp*, CN, ON, NeNa, and MgAl cycles, exhibit star-to-star abundance variations, far in excess of the modest variations seen in halo field stars (see, e.g., Sneden 1999, 2000; Gratton et al. 2004). In some cases these abundance spreads are seen in stars near the turnoff and along the subgiant branch (e.g., Gratton et al. 2001), suggesting that these anomalies arise from some process of self-enrichment occurring at the first stages of cluster life. This is generally attributed to pollution from the winds of the massive asymptotic giant branch (AGB) objects (e.g., Cottrell & Da Costa 1981; D'Antona et al. 1983; D'Antona 2003), whose convective envelopes are subject to hot bottom burning (HBB) (e.g., Ventura et al. 2001, 2002). So these envelopes are an ideal environment for the manufacture of elements through nuclear reactions in which proton captures are involved.

While problems persist in obtaining a quantitative reproduction of the observed abundance spreads (Denissenkov & Herwig 2003; Ventura et al. 2004; Fenner et al. 2004; Ventura & D'Antona 2005a), a high helium abundance in the ejected matter is a robust prediction of the models (Ventura et al. 2001, 2002). D'Antona et al. (2002) have shown that the hypothesis that GC stars were formed in two different star formation events can explain the presence of long blue tails in the horizontal branches (HBs) in GCs with large abundance anomalies (Catelan & de Freitas Pacheco 1995). In their scenario the bluer HB stars are born from the helium-rich stellar population. In addition, D'Antona & Caloi (2004) have shown that the peculiar bimodal distribution of stars in the cluster NGC 2808 can be explained in the same way, by assuming that the cluster composition today is about half stars belonging to the first stellar generation and about a half born from the AGB winds, whose initial helium abundance is larger than $Y \simeq 0.27$ and extends up to $Y \simeq 0.35$.

The suggestion that helium is a possible second parameter for globular cluster stars (see Rood 1973, Rood & Crocker 1989, and Fusi Pecci & Bellazzini 1997 for a general overview) has been reinforced by the discovery that the complex object ω Cen has at least two different components of the main sequence (MS) and multiple turnoffs (TOs) (Bedin et al. 2004; Ferraro et al. 2004) and that the bluer MS can be explained by a metal- and helium-enriched population (Norris 2004).

In contrast to ω Cen, NGC 2808 does not show a metallicity spread (Carretta et al. 2004). The comparison of isochrones differing in helium for the TO and MS in D'Antona & Caloi (2004) showed that it is not easy to dismiss the hypothesis of differences in helium content among NGC 2808 stars. Indeed, they predicted that one could observe a color bifurcation in the MS and/or in the subgiant branch if there are at least two

¹ INAF—Osservatorio Astronomico di Roma, via Frascati 33, 00040 Monteporzio, Italy; dantona@mporzio.astro.it.

² INAF—Osservatorio Astronomico di Bologna, via Ranzani 1, 40127 Bologna, Italy; michele.bellazzini@bo.astro.it, flavio.fusi.pecci@bo.astro.it.

³ INAF—Istituto di Astrofisica Spaziale e Fisica Cosmica, via Fosso del Cavaliere, 00133 Rome, Italy; vittoria.caloi@rm.iasf.cnr.it.

⁴ Department of Astronomy, University of Virginia, Charlottesville, VA 22903-0818; rtr@virginia.edu.

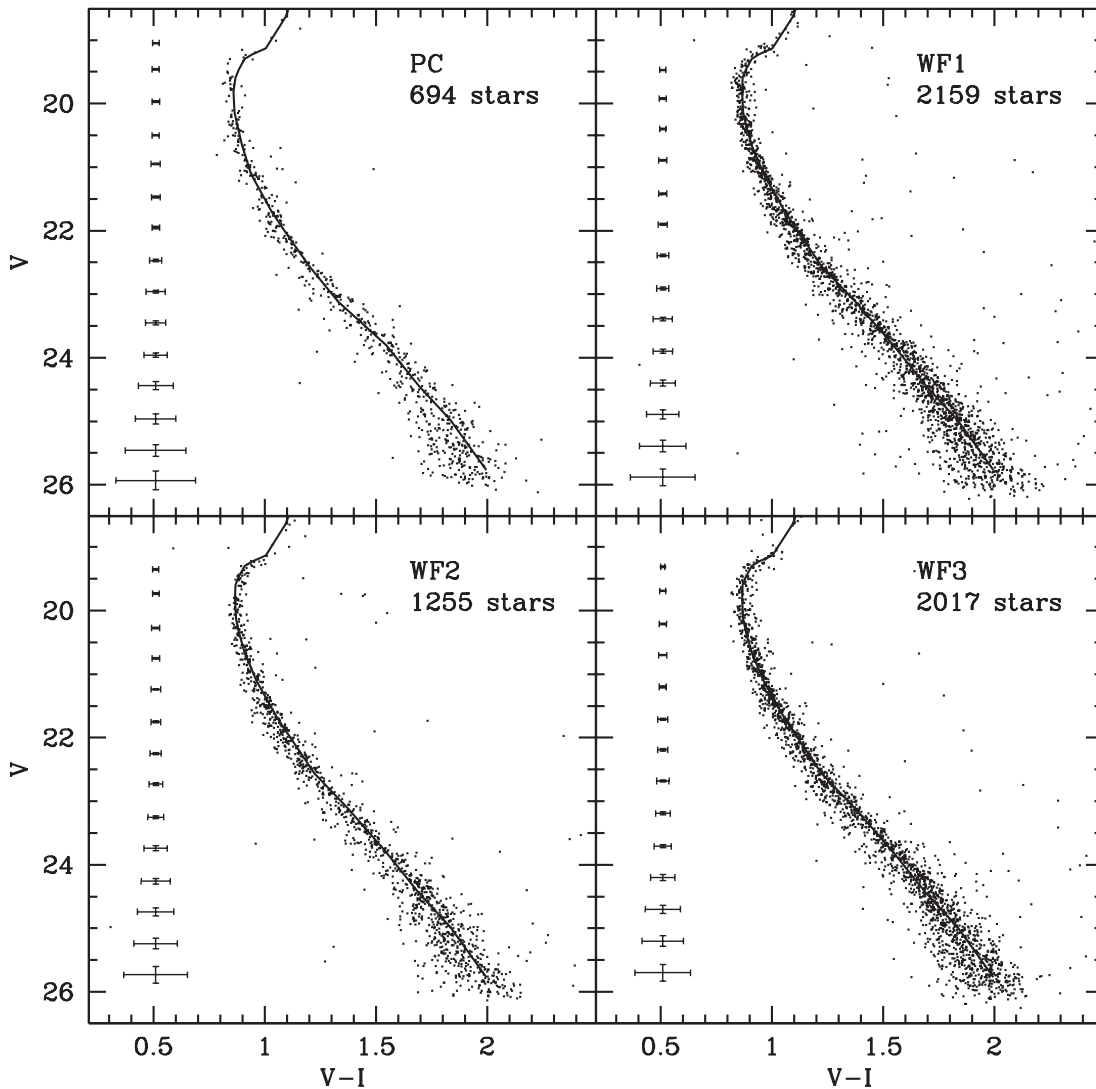


FIG. 1.—CMDs from the four WFPC2 cameras. The error bars have been obtained from the artificial-star experiments [$\sigma_V = V_{\text{output}} - V_{\text{input}}$ and $\sigma_{V-I} = (V-I)_{\text{output}} - (V-I)_{\text{input}}$]. The ridge lines of each sample are overlotted.

homogeneous groups of stars with different helium abundances. To investigate this possibility, we have used *Hubble Space Telescope* (*HST*) WFPC2 photometry of a field in the outskirts of NGC 2808 to obtain a deep, high-precision color-magnitude diagram (CMD) of the main sequence. Since we were searching for a spread in the sequences, we also performed an extensive error analysis.

We find that $\sim 20\%$ of the MS stars of the cluster lie to the blue of the bulk of the MS. The blue outliers must be due to an intrinsic difference between the stars (§ 2). In §§ 3 and 4 we suggest an interpretation of these anomalous MS stars *and* of the HB morphology of the cluster within the context outlined above. In § 5 we discuss and summarize the results.

2. OBSERVATIONAL RESULTS

We reduced a data set of four $t_{\text{exp}} = 900$ s plus three $t_{\text{exp}} = 100$ s F555W images and four $t_{\text{exp}} = 700$ s plus three $t_{\text{exp}} = 120$ s F814W images, obtained with the WFPC2 on board *HST*. The images were acquired by adopting a dither pattern that allows a virtually total cleaning of cosmic-ray hits and chip defects. The field is located at $\simeq 4.5$ from the center of the NGC 2808 (GO 06804). The field samples the outskirts of the cluster, at ~ 17 core radii (r_c) and ~ 6 half-light radii from the center (Trager et al.

1993), and it appears relatively uncrowded when imaged with the superb spatial resolution of the WFPC2. This allowed us to obtain excellent photometry down to the faintest detectable stars, since source confusion was not a concern. The prerduced (flat, bias) images provided by the Space Telescope Science Institute were reduced individually with HSTPHOT (Dolphin 2000), a point-spread function–fitting package specifically suited for WFPC2 images. HSTPHOT automatically provides accurately calibrated and CTE-corrected photometry. In the following we refer only to the photometry calibrated in the Johnson-Kron-Cousin system, hence in V and I instead of F555W and F814W.⁵ The adopted threshold for source detection on the frame was 3σ above the background. For each filter, the four catalogs from the long-exposure images were cross-correlated, and the average of the individual measures was taken as the final magnitude estimate, as well as the standard deviation as an estimate of the photometric error. Only stars that were detected and successfully measured in at least three images were retained in the final catalog of average magnitudes. We proceeded in the same way for the short-exposure images, in this case the retained sources were present in

⁵ The results we present also hold if we maintain the flight system colors; that is, they are not an artifact of the color transformations.

at least two images. The V and I catalogs of the long and short exposures were then coupled and finally the V and I long and short catalogs were merged after careful relative photometric calibration. In the final global catalog, all the sources with $V > 20.0$ are from the long exposures and those with $V \leq 20.0$ are from the short ones. Note that the results presented in the following are based exclusively on stars with $V > 20.0$, hence those extracted from the homogeneous set of the long-exposure images. Note also that the selection criteria described above ensure that the final data set is essentially free of spurious sources, since only stars with at least three measurements in V and three measurements in I are included in the final catalog, for $V > 20.0$.

2.1. Color Magnitude Diagrams and Artificial-Star Experiments

The CMDs obtained from each WFPC2 camera are shown separately in Figure 1. The points of the overplotted ridge lines have been obtained as 2σ clipped averages in color over 0.2 mag boxes, as described in Ferraro et al. (1999). For each of the four subsamples (PC, WF1, WF2, and WF3) we derived a separate ridge line to account for any subtle camera-to-camera systematic difference in the photometry. Such effects typically amount to ± 0.01 mag. A ridge line for the total sample has also been derived with the same technique.

The CMDs are clearly dominated by the narrow and well-defined cluster sequences: the subgiant branch (SGB) and the base of the red giant branch (RGB) for $V < 19.5$, the TO point around $V \simeq 20.0$, and the MS going from $(V, V - I) \simeq (20.0, 0.8)$ to $\simeq (26.0, 2.0)$. A handful of foreground Galactic stars is visible in the CMDs of the WF cameras, a couple of magnitudes above the cluster MS. A sparse sequence running parallel to the MS, ~ 0.1 – 0.2 mag to the red of it, may be due to a mix of blended MS stars and real binary systems (see Bellazzini et al. 2002 and references therein).

On the other hand, there is a sizable fraction of MS stars scattered to the blue of the ridge lines, and no obvious observational effect can be responsible for pushing a cluster star in this direction. It is worth noting that while HSTPHOT should be the ideal choice for the present application, we repeated the data reduction using DoPHOT (Schechter et al. 1993), following the prescriptions by Bellazzini et al. (2002), and SExtractor (Bertin & Arnouts 1996). The unexpected blue stars appeared the same in the CMDs obtained with these codes, and hence their anomalous color cannot be due to some subtle effect associated with the reduction process. These blue MS stars are the main subject of the following subsections.

To accurately characterize all the effects due to the observations plus data reduction processes and to have an idea of the completeness of our sample, we performed an extensive set of artificial-star experiments on one V and one I image from the long-exposure set. The artificial stars were distributed according to the observed spatial distribution and luminosity function, as described in Dolphin (2000), and were added simultaneously in the V and I frame at the same position; hence, artificial stars have a properly defined $V - I$ color (as in Bellazzini et al. 2002). In several runs we accumulated a total of 91,680 artificial stars, 30,221 of which have input magnitudes and colors within ± 0.15 mag of the cluster ridge line, which we refer to as the ‘‘Similar Sample.’’ We used the latter subsample to study in more detail the MS stars we are interested in. The average of $V_{\text{output}} - V_{\text{input}}$ and that of $(V - I)_{\text{output}} - (V - I)_{\text{input}}$, computed in ~ 0.5 mag boxes, were taken as the typical photometric errors in magnitude and color, respectively, and are plotted as error bars in the various panels of Figure 1. The average errors derived

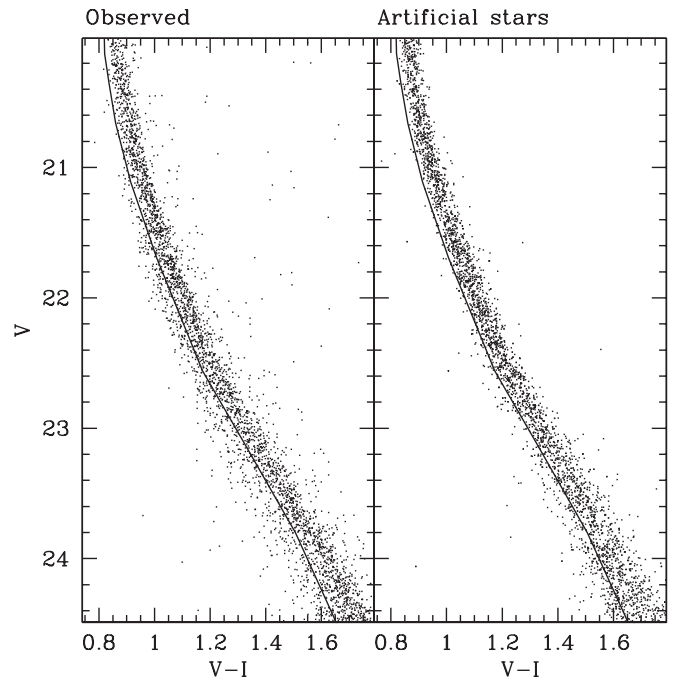


FIG. 2.—*Left*: Zoomed view of the total CMD (four chips). *Right*: Synthetic CMD obtained from the artificial-star experiments. The MS ridge line overplotted on both diagrams has been shifted by -0.05 mag in color.

from the artificial-star experiments are in excellent agreement with the standard deviations obtained from the repeated measures described in § 2.

The completeness is greater than 80% for $V \leq 25.0$ for all of the considered subsamples. Since we limit the following analysis to $V \leq 24.0$, we are well within a nearly constant completeness regime, more than 1 mag brighter than the limit at which the completeness begins to fall rapidly to zero (around $V \sim 25.5$). The derived completeness function slightly overestimates the actual completeness, because of the severe selection criteria applied to the observed sample; nevertheless, it gives a clear indication of the magnitude range in which completeness is high and essentially constant with magnitude. Analogously, the photometric uncertainty as estimated from the artificial stars is in principle slightly larger than the actual values, since in the observed sample each magnitude is the average of at least three independent measures. However, it provides an independent check on the photometric accuracy and very stringent constraints on the *distribution* of photometric errors, for instance on the symmetry between the errors that make a given star bluer or redder than it was in input (see below).

2.2. Blue Main-Sequence Stars

In Figure 2 we compare the observed global CMD (stars from all the cameras) with a CMD with the same number of stars randomly extracted from the Similar Sample of artificial stars.

The synthetic CMD in the right panel of Figure 2 was obtained as follows: (1) each extracted star was assigned the color of the cluster ridge line at the corresponding V_{input} by spline interpolation; (2) the corresponding $(V - I)_{\text{output}} - (V - I)_{\text{input}}$ (positive or negative) was added to the assigned color; (3) V_{input} was substituted by V_{output} . In this way we reproduce the effects of observations plus data reduction on a parent population of stars that were exactly placed on the cluster ridge line, as in Bellazzini et al. (2002). In both panels, for reference, we also

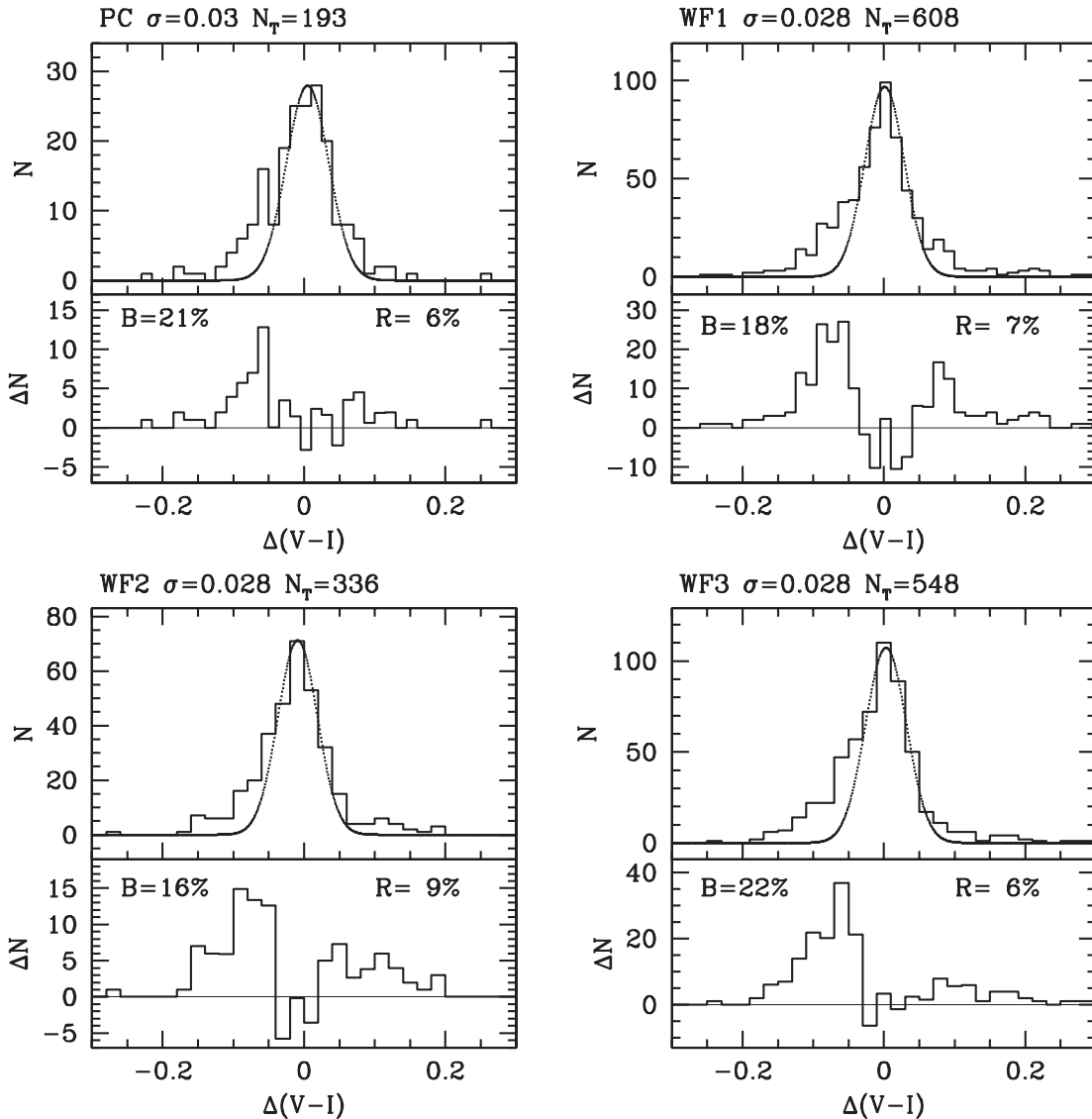


FIG. 3.—Distributions of the color deviations from the ridge line for the stars having $22.0 < V < 24.0$ in the four samples shown as histograms in the top part of each panel. The dotted lines are Gaussian curves fitting the core of the observed distributions. The adopted σ -values are the typical σ_{V-I} obtained from the artificial-star experiments. The bottom part of each panel shows the residuals of the subtraction of the Gaussian model from the observed distribution of deviations. The fractions of residual stars having $-0.2 \leq \Delta(V-I) < 0.0$ (B) and $0.0 < \Delta(V-I) \leq 0.2$ (R) are also reported.

show the ridge line of the global sample shifted by -0.05 mag in $V-I$.

The comparison between the observed and synthetic CMDs shows that the excess of stars to the blue and to the red of the MS described above cannot be due to observational effects but, instead, is intrinsic to the observed sources. Hence, the observed population must include (1) a nonnegligible fraction of real binary systems that appear as the usual parallel sequence to the red of the MS and (2) a significant population of stars scattered blueward of the MS in the whole sample from $21.0 \leq V \leq 24.0$. The origin of this anomalous blue MS population is unknown.

In order to quantify the frequency of the blue MS stars, in Figure 3 we show the distribution of color deviation from the cluster ridge lines [$\Delta(V-I)$], separately for each subsample (camera), in the range in which the effect is more clearly visible ($22.0 \leq V \leq 24.0$). To disentangle the various components of the MS, we subtract from the observed distributions Gaussian curves with σ equal to the typical error in color in that magnitude range. These Gaussians fit well the core of the distributions

as shown by the small residuals in the few central bins. The residuals of the subtractions having $-0.2 \leq \Delta(V-I) < 0.0$ are divided by the total number of stars in the distribution to obtain the fraction of blue stars (B), and the same is done for the $0.0 < \Delta(V-I) \leq 0.2$ residuals (R). The population of blue MS stars clearly emerges in all the samples as a distinct bump in the residuals containing $\sim 20\%$ of all of the MS stars in the considered magnitude range.

It is interesting also to compare, in the same magnitude range, the symmetry properties of the observed color deviations from the ridge line with those derived from the artificial stars shown in Figure 2. In this case we call B the number of stars having negative $\Delta(V-I)$ and R the number of those with positive $\Delta(V-I)$. The total observed sample has $(B-R)/(B+R) = 0.12 \pm 0.02$, clearly indicating an excess of blue stars, while the deviations of the artificial-star sample are extremely symmetric, having $(B-R)/(B+R) = 0.01 \pm 0.01$. The difference between the two values is significant at the 4.4σ level. Analogously, we find $B/R = 1.26 \pm 0.06$ for the observed sample, compared with $B/R = 1.01 \pm 0.02$ for the synthetic one.

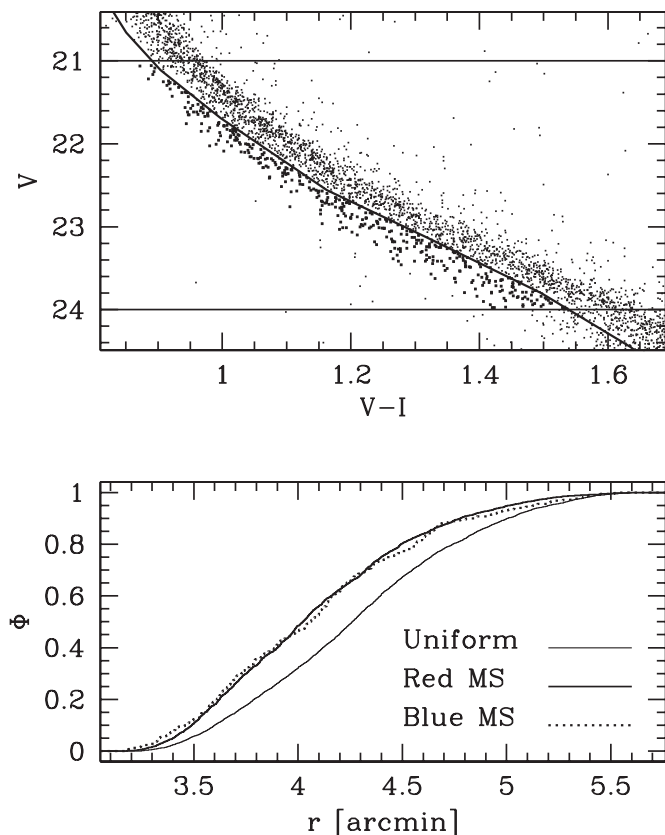


FIG. 4.—*Top*: Selection of blue MS (to the blue of the shifted ridge line, square dots) and red MS stars (to the red of the shifted ridge line). The horizontal lines enclose the magnitude range of the adopted selections. *Bottom*: Cumulative radial distributions of blue (dotted line) and red (solid line) MS stars.

2.3. A Possible Role for Differential Reddening?

The interstellar extinction toward NGC 2808 is quite large for a halo GC ($A_V = 0.68$ mag; Harris 1996), and hence we address the question of whether small-scale variations of reddening could lead to the observed difference in color among MS stars (blue vs. “normal” MS). Two pieces of observational evidence argue against this hypothesis. First, blue MS stars are evenly spread over the whole field and do not show any particular clustering property (see also Fig. 4 below; however, this is not a strong argument, as the interstellar dust is distributed in sheets and filaments and may vary on angular scales of arcseconds). Second and more relevant, the color spread along the MS occurs only for $V \geq 21.0$ (see Figs. 1 and 2). If differential reddening were the cause of the color spread, we would observe it in any region of the CMD, and in particular, it should be very evident in the nearly vertical portion of the sequence around the TO point ($V \simeq 19.5\text{--}20.0$). On the contrary, the MS is clearly unimodal there and displays a color distribution fully compatible with what is expected from the photometric errors alone (see Fig. 2).

Given the above evidence, we conclude that the anomalous population of blue MS stars is not due to the presence of differential reddening in the (small) field considered here.

2.4. Radial Distribution

While the sampled field is so small ($<2.6 \times 2.6$) that the contamination by any possible system other than the cluster itself should be negligible, the membership of the blue MS stars to NGC 2808 must be established. This is particularly relevant

in the present case, since the cluster may be physically associated with the newly discovered Canis Major galaxy (Martin et al. 2004), which in any case is projected in the same area of sky as this stellar system, whose optical CMD displays a narrow and well-defined MS with a TO around $V \simeq 19.0$ (Bellazzini et al. 2004; Martinez-Delgado et al. 2005). The only way to assess this point with our data is to compare the radial distribution of blue MS stars with that of ordinary MS cluster stars.

If blue MS stars are cluster members, they must be distributed like any other star in NGC 2808; if, on the contrary, they belong to a system with a much larger size (such as Canis Major or any known Galactic component), their spatial distribution should be approximately uniform over the observed field.

The results of this test are shown in Figure 4. In the top panel we show the adopted selection, stars to the blue and to the red of the shifted ridge line, while the cumulative radial distributions are displayed in the bottom panel. The distribution of blue MS stars is indistinguishable from that of normal MS cluster members and differs strongly from a uniform distribution over the considered field. According to a Kolmogorov-Smirnov test, the probability that the blue MS sample is drawn from a uniformly distributed population is $P = 3.4 \times 10^{-10}$. Hence, blue MS stars must be associated with NGC 2808.

In conclusion, we have observationally established that $\sim 20\%$ of genuine MS stars of NGC 2808 are intrinsically bluer than the main locus of most of the other MS stars of the cluster. In the following sections we suggest an interpretation of this unexpected and puzzling observational result.

3. THE THEORETICAL MODELS AND THE SIMULATIONS

We computed new HB models, in addition to those presented in D’Antona & Caloi (2004), namely, the models with $Y = 0.40$. The core mass at the helium flash for GC ages (12–13 Gyr) is in this case $M = 0.465 M_\odot$, compared to $M = 0.495 M_\odot$ for $Y = 0.24$. Extreme HB stars in which only core helium burning is active, with the H shell not contributing to energy generation, are about 0.4 mag fainter for $Y = 0.40$ than for $Y = 0.24$. HB stars with $Y = 0.40$ can extend to the faintest blue clump of the HB of NGC 2808, by assuming an H envelope of the order of $10^{-3} M_\odot$ around the helium-burning core of $0.465 M_\odot$ (ZAHB luminosity $\sim 1.16 L_\odot$, $T_{\text{eff}} \sim 31,500$ K; see Fig. 5). Synthetic models for the HB are computed following the procedure described by D’Antona & Caloi (2004).

For the MS study, we computed stellar models down to $0.3 M_\odot$, to construct isochrones for metallicity $Z = 10^{-3}$ and helium content $Y = 0.24, 0.28, 0.32$, and 0.40 and for metallicity $Z = 2 \times 10^{-3}$, for $Y = 0.24, 0.30$, and 0.40 . The input physics is described in D’Antona & Caloi (2004). Models for $M < 0.4 M_\odot$ are built by using a new equation of state based on Saumon et al. (1995), Rogers (2001), and Stolzmann & Blöcker (1996, 2000) computations.

Synthetic models for the cluster MS, TO, and subgiant population are built by interpolating among the isochrones with various assumptions about the helium content. We fix the age of the cluster, and the stellar mass is randomly extracted from a power-law mass function (results are shown for an exponent -1.5 , in the notation in which the Salpeter index is -2.3 ; in any case, the choice of the mass distribution has no influence for the specific problem of this work). The number of stars for each chosen helium content is fixed a priori, and the resulting color distribution is compared with the observations to choose the most appropriate ones. After each determination of magnitude and color, we

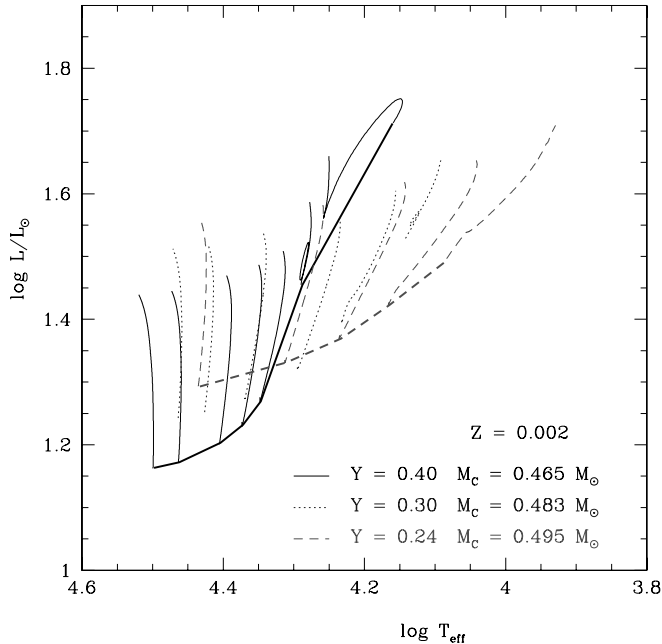


FIG. 5.—Evolutionary tracks for the hottest region of the HB. Tracks are terminated when the core helium content is reduced to $Y = 0.10$. From left to right, masses are 0.5, 0.52, 0.54, 0.56, and $0.58 M_{\odot}$ ($Y = 0.24$); 0.486, 0.49, 0.50, 0.52, 0.54, and $0.56 M_{\odot}$ ($Y = 0.30$); 0.466, 0.469, 0.48, 0.49, 0.50, 0.52, and $0.54 M_{\odot}$ ($Y = 0.40$). For $T_{\text{eff}} \geq 20,000$ K, the $Y = 0.40$ ZAHB is less luminous than the ZAHB for $Y = 0.24$, because of the reduced helium core mass. At $T_{\text{eff}} \leq 20,000$ K, the contribution of the H shell burning to the luminosity begins to be relevant, and the effect is more important for larger Y (see, e.g., the luminosity of $M = 0.52$ and $0.54 M_{\odot}$ for $Y = 0.40$). Heavy solid line: ZAHB with $Y = 0.40$; heavy dashed line: ZAHB with $Y = 0.24$. [See the electronic edition of the Journal for a color version of this figure.]

apply an error extracted from a normal distribution with standard deviation chosen according to the observations.

In running the simulations of the MS color distribution we employed the following procedure: we first took the distribution of a sample of stars with standard helium abundance $Y = 0.24$, then we added stars with increasing helium content in order to reproduce reasonably the observed distribution in color. Our first aim is to reproduce the MS, including the blue MS stars. At the same time, we have also to worry about the observed HB morphology. Therefore, we finally adopt helium distributions $N(Y)$ such that they are consistent both with the MS colors and with the two main features of the HB, the gap at the RR Lyrae and the distribution of stars in the EBT1 and EBT2+EBT3 blue clumps (we follow the definitions by Bedin et al. 2000). Of course, no $N(Y)$ that reproduces the HB but not the MS colors is allowed, and vice versa. We ran simulations for both $Z = 10^{-3}$ and 2×10^{-3} , finding similar results for the MS color distribution.

We show in Figure 6 a simulation of the TO and MS, made according to the method described above, in which the $N(Y)$ follows the distribution given in Figure 9, which is discussed in § 3.1. We superimpose the isochrones of 13 Gyr, $Z = 2 \times 10^{-3}$. A look at Figure 6 shows an important feature. The theoretical isochrones with variable helium and fixed age converge at the TO region. This implies that if helium variations are responsible for the blue MS subsample, significantly bluer than the MS ridge line and fainter than the TO, the intrinsic dispersion of the data at the TO should be negligible and due just to photometric errors. Examination of Figures 1 and 2 shows that this is indeed the case. The TO region in the CMD of NGC 2808 ($19.5 < V < 20.5$) is vertical and extremely narrow in color, and essentially no blue outlier is detectable.

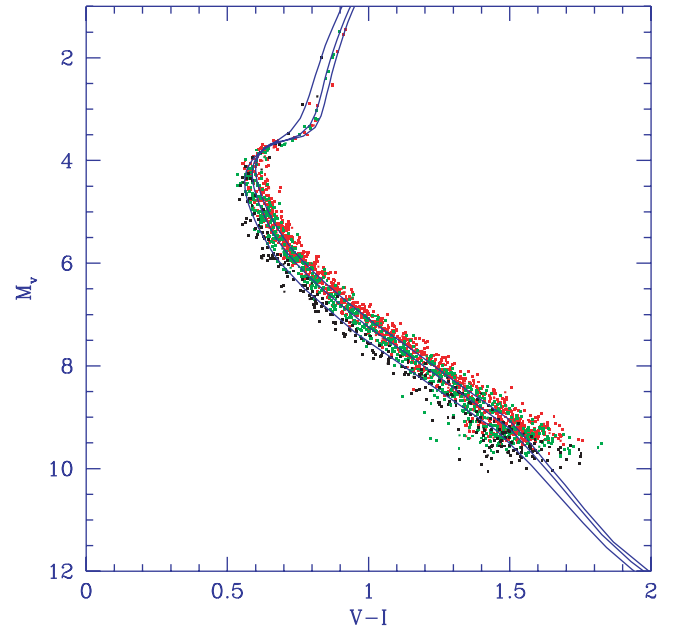


FIG. 6.—Three isochrones with age 13 Gyr, $Z = 2 \times 10^{-3}$, and $Y = 0.24$, 0.30, and 0.40. The simulation based on these three isochrones has the $N(Y)$ shown in Fig. 9. The standard deviation in color σ added to the simulation is fixed on the basis of the observational errors, which increase with the magnitude.

3.1. The Distribution in Color: The MS

In Figure 7 we show the color distribution corresponding to the simulation in Figure 6, in the magnitude range $5.5 < M_v < 7.5$. In order to reproduce the MS observations, it would suffice to consider simply two helium values: $Y = 0.24$ for the vast majority of stars ($\sim 80\% - 85\%$) and $Y \sim 0.40$ for the remaining fraction. However, in the simulation, we do not assume a unique $Y = 0.24$ for this main fraction of stars because of the necessity of reproducing the HB morphology, but the $N(Y)$ shown in Figure 9 for $0.24 \leq Y \leq 0.29$. The small additional scatter in the MS is consistent with the observed color distribution having observed standard deviation $\sigma = 0.03$, which means that it remains hidden within the photometric errors. This follows from the fact that in the models,

$$\frac{\Delta(V-I)}{\Delta Y} \simeq -0.438. \quad (1)$$

Thus, the color of stars having, e.g., $Y = 0.275$ is shifted with respect to an MS with $Y = 0.24$ only by -0.015 mag.

According to equation (1), the blue MS can be reproduced only by adding a group of stars (from $\sim 15\%$ to $\sim 22\%$; see Fig. 3) with $Y = 0.40$. This additional group of stars is absolutely necessary—in fact, had we adopted a more or less uniform spread in helium, it would have produced too many stars at $\delta(V-I) \simeq -0.05$ and not enough stars at $\delta(V-I) \simeq -0.10$. The specific value $Y = 0.40$ should not be taken as a precise quantitative estimate, as our models suffer from at least one important uncertainty: the color versus T_{eff} relationships are based on models by Bessell et al. (1998), which are built with normal helium content.

3.2. The Distribution in Color: The HB

The $N(Y)$ distribution illustrated above and displayed in Figure 9 is chosen in order to reproduce the HB morphology at a first-order approximation. In particular, it allows us to obtain the observed lack of HB stars in the RR Lyrae region and the distribution of stars of the clump EBT1 (Bedin et al. 2000). In

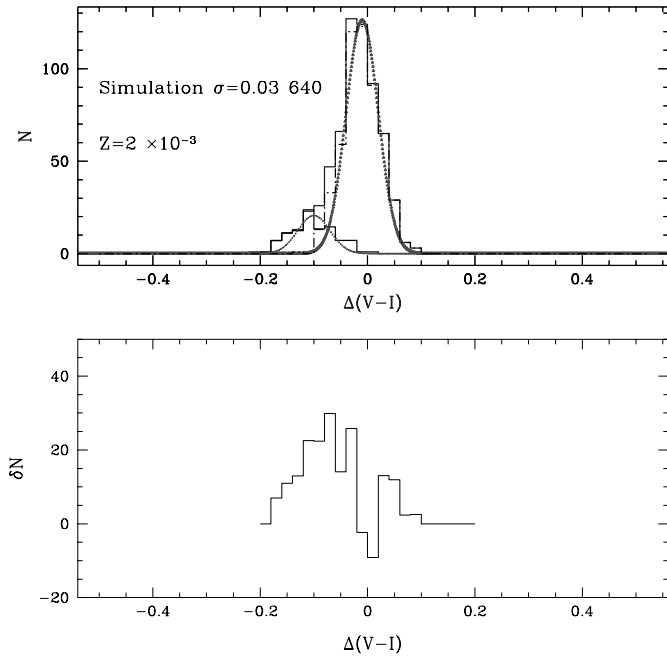


FIG. 7.—Color distribution of the MS stars in NGC 2808 in the field WF3. The stars are limited to the range between $M_p = 5.5$ and 7.5 . The Gaussian fit with the same standard deviation as the data ($\sigma = 0.03$) shows an excess of stars at blue colors. The observed distribution, extended to the blue up to -0.2 mag from the median line, requires a distinct population with high helium to be reproduced. This population at $Y = 0.40$, including about 15% of the total stellar population in this MS range, is shown separately by the histogram at the left, fitted with a Gaussian. The dash-dotted histogram includes the stars with helium content up to $Y = 0.29$. The bottom panel shows the differences between the simulation counts and the Gaussian expected values. [See the electronic edition of the *Journal* for a color version of this figure.]

summary: (1) $\sim 15\%$ of the stars have $Y = 0.40$; these stars account for the blue MS population and populate the EBT2 and EBT3 clumps of the HB; (2) $\sim 50\%$ of the stars have $Y = 0.24$; and (3) $\sim 35\%$ of the stars have Y in the range $0.26 < Y < 0.29$. The addition of the latter stars—not required by the observed MS morphology—does not significantly worsen the MS fit, as discussed above. Figure 8 shows that it also reproduces quite satisfactorily the HB general morphology. The comparison of the full HB simulation is made with the Bedin et al. (2000) observations.

The interesting result from the global simulation is that the reproduction of the MS color distribution, coupled with a good description of the whole HB morphology, naturally leads us to the conclusion that about 15%–20% of the cluster stars have a helium content of ≈ 0.4 and show up *both* in the MS color distribution (Fig. 7; the bluest MS stars) *and* in the HB, where they are present in the two blue HB tails, EBT2 and EBT3.

Note that we cannot reproduce the gap between EBT2 and EBT3, but only the total number of stars. However, it is not straightforward to obtain the correct star distribution in these two HB regions. If we interpret observations in terms of mass distribution of stars with $Y = 0.40$, we find that the population in EBT3 arises from only one mass, of about $0.466 M_\odot$, which evolves vertically (see Fig. 5) at a more or less constant pace, covering the observed faintest blue region. A spread in mass necessarily fills the gap between EBT3 and EBT2.⁶ For the latter

⁶ Lee et al. (2005) attribute the EBT2 and EBT3 clumps to two populations differing in helium content, but they do not explain why each of these should have practically a unique evolving mass.

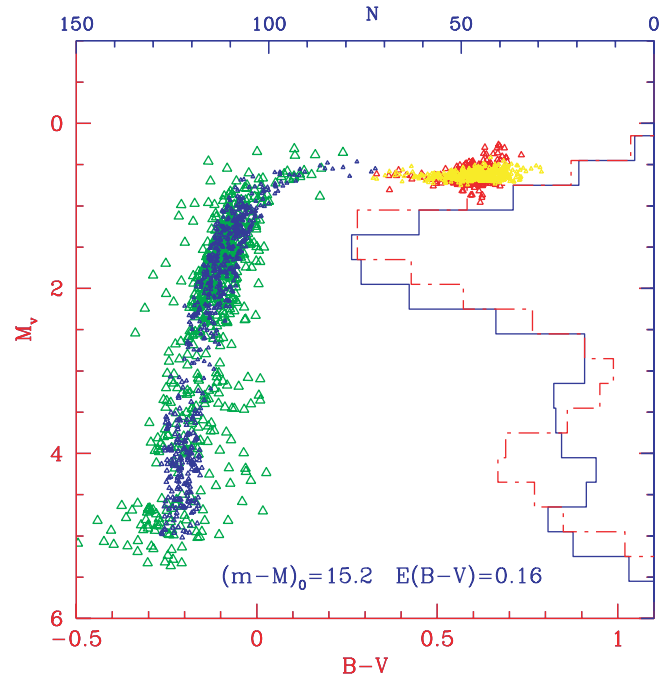


FIG. 8.—By assuming the same helium distribution (Fig. 9), which reproduces the MS colors, in addition to some assumptions relative to the mass loss, we obtain a synthetic HB distribution, compared here to the observed data for the cluster NGC 2808 by Bedin et al. (2000). The red clump is made up by stars with $Y = 0.24$, the blue clump EBT1 (the most conspicuous and luminous) contains stars with $0.26 < Y < 0.29$, with a strong prevalence of stars at $Y = 0.27$ – 0.28 ; the clumps EBT2 and EBT3 contain the stars with $Y = 0.40$.

group of stars the situation is not very different: the bulk of it is confined between 0.48 and $0.49 M_\odot$. A possible interpretation is to consider EBT2 stars as deriving from red giants, which develop the helium flash at the tip of the giant branch, that is, “normal” HB stars. With an evolving giant of about $0.63 M_\odot$, the mass loss involved amounts to about $0.15 M_\odot$ and the envelope mass to about $0.015 M_\odot$, sufficient for a standard helium flash. Larger mass losses would give rise to early or late hot flashers, as defined and discussed by Castellani & Castellani (1993), D’Cruz et al. (1996), and Brown et al. (2001), that is, stars in which the core-helium flash takes place, either at the beginning or later, along the white dwarf cooling sequence. In this respect, a fundamental piece of information comes from the observations by Brown et al. (2001) and Moehler et al. (2004). In particular, Moehler et al. (2004) obtained spectra of EBT3 members, finding evidence both of the high surface temperatures (35,000 K and more) and of the large surface abundance of helium and carbon, expected as a consequence of the mixing during the late core-helium flash (Sweigart 1997). This appears to decisively settle the question of the origin of these stars.

On the other hand, the simulation shown in Figure 8 has a problem: we have to assume a mass loss of $\sim 0.195 M_\odot$ during RGB evolution in order to reproduce the red side of the HB with $Y = 0.24$ models and the clump EBT1 with the assumed $N(Y)$. Then the mass loss has to be reduced to only $\sim 0.15 M_\odot$ to account for the extreme blue tails with $Y = 0.40$. If the mass-loss regime does not change too much with helium content, the $Y = 0.40$ evolving giants should leave the giant branch before reaching the conditions for the core-helium flash. On the contrary, the difference between the fraction of blue MS stars and the fraction of EBT2+EBT3 stars may amount to $\sim 5\%$, according to Bedin et al.’s (2000) and our own observational estimates. This is just one of the many questions and problems that this exploratory

investigation leaves open. If the helium content of the blue MS could be reduced to $Y \sim 0.35$, the mass-loss problem would be practically solved. We have already noted the uncertainties in the color- T_{eff} transformations, which might depend on Y , that are not taken into account in the model atmospheres.

At this stage we cannot pretend to explore all the details of the HB morphology of this cluster, as there are a number of parameters (mass loss included) that certainly influence it (Rood 1973; Fusi Pecci et al. 1993; Fusi Pecci & Bellazzini 1997). Nevertheless, we stress that the quantitative reproduction of the main anomalies, both of the MS (blue MS stars) and of the HB (red HB, gap at the RR Lyrae, blue HB with extreme blue tails), indicates that the proposed interpretation in terms of helium variations is one of the most promising proposed thus far.

4. THE STAR FORMATION EVENTS IN NGC 2808: A NEW GLOBAL SCENARIO

The results of this work provide new information on the early stages of star formation in GCs. In D’Antona & Caloi (2004) we hypothesized more or less continuous star formation starting after the period of Type II supernovae explosions. After a few times 10^7 yr the slow winds from massive AGB stars would begin to collect helium-enriched material in the cluster core and form stars.

Figure 9 shows the comparison between the $N(Y)$ suggested in D’Antona & Caloi (2004) and that derived in this work. The latter seems to depict a situation very different from continuous star formation. However, it is to be preferred, since the MS color distribution is a much better determinant than the HB distribution for deriving $N(Y)$. The HB distribution depends on many parameters other than Y , so it can never yield a unique $N(Y)$.

The HB distribution does suggest that NGC 2808 probably underwent three main stages of star formation. The *first* one is easily identified with the main burst of star formation and is now probed by the low-mass stars with primordial helium content ($Y = 0.24$), which constitute $\sim 50\%$ of the MS and populate the red HB clump. The *second* burst in chronological order results in the 15%–20% share of the population at $Y = 0.40$. Finally, there is a *third* stage of star formation, producing $\sim 30\%$ – 35% of the stars with helium content greater than the primordial value, up to about $Y = 0.29$. These stars populate the HB clump EBT1.

The reason why the stars from the second burst of formation have the highest Y is simply that the helium content in the AGB envelopes increases with the initial stellar mass, due to the higher efficiency of the second dredge-up (Ventura et al. 2002). Ventura & D’Antona (2005b) estimate $Y = 0.32$ for their most massive models ($6.5 M_{\odot}$) for metallicity $Z = 10^{-3}$. This value can be considered conservative, as their models do not include any kind of overshooting, which may easily increase the helium content to the required value of $Y = 0.40$. Lattanzio et al. (2004) find $Y \sim 0.36$ from the evolution of a $6 M_{\odot}$ with $Z = 0.004$. In addition the episodes of the third dredge-up may help to increase the helium content in some models (Ventura & D’Antona 2005a). Note also that $Y \sim 0.35$ would reduce the problems in the reproduction of the blue tails EBT2 and EBT3 (see § 3.2). Therefore, we suggest identifying the population with extreme helium abundance ($Y \sim 0.40$) as the stars born from the winds of the *most massive* AGB stars, which evolve ~ 50 Myr after the first burst of star formation.

The third group of stars may be the result of star formation from the winds of somewhat smaller mass AGBs. If we rely on the AGB models by Ventura et al. (2002), the best mass range for these objects is from $\lesssim 4.5$ to $\gtrsim 3.5 M_{\odot}$, which evolve at ages ~ 100 – 150 Myr after the first burst of star formation. Hence, the

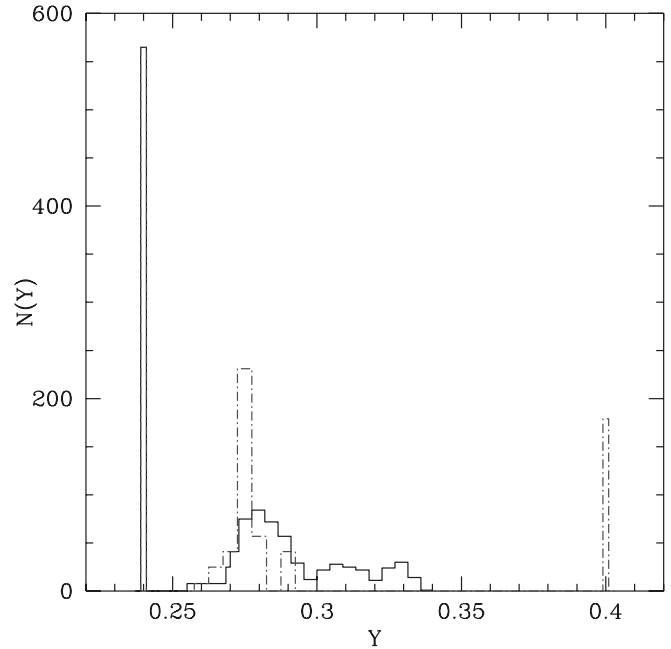


FIG. 9.—Helium distribution adopted for the simulation shown in Figs. 7 and 8 (dash-dotted line) compared with the helium distribution predicted by D’Antona & Caloi (2004) for the HB (solid histogram). [See the electronic edition of the Journal for a color version of this figure.]

“intermediate” helium-rich stars represent the third stage of star formation in chronological order.

We are aware that this scenario requires an initial mass function of the first burst of star formation strongly weighted toward intermediate-mass stars, in order to get the necessary amount of helium-enriched ejected matter. This aspect of the problem has been extensively discussed in D’Antona & Caloi (2004).

4.1. The Possible Role of Delayed Type II Supernovae Explosions in Binaries

In our scenario there are no stars formed with helium $0.29 < Y < 0.40$. Naively one would expect that as the cluster ages, the mass of the AGB stars decreases, as does the helium abundance in the winds and in the newly born stars. If the formation of new stars is continuous, why do we not observe stars with all Y -values between 0.29 and 0.40? We briefly consider three possible answers.

First, our modeling of AGB stars is not so secure as to exclude discontinuities in the helium content of the AGB ejecta. In fact, some of the models (Ventura et al. 2002, Fig. 4) show a nonlinear correlation between the evolving mass and the helium yield. Depending on the efficiency of star formation, on the modalities of mixing of the intracluster material ejected from the AGBs, and on the initial mass function of the AGB stars, there could be a relative rarity of stars in some helium abundance ranges.

Second, it is possible that external events are needed to trigger the star formation phase. In this case, after a first trigger when $Y = 0.40$, the gas from the AGB ejecta goes on accumulating in the cluster central regions for a long time (several tens of millions of years) until the second trigger occurs when the average helium content in the gas is reduced to $Y \sim 0.28$.

A third possibility requires a bit more explanation. The uniform metallicity of GC stars is generally attributed to the fact that the explosion of Type II supernovae do not pollute the gas from which the stars are formed, probably because they bring an end to the first burst of star formation by clearing from the gas

the intracluster medium. Type II supernovae continue until all single stars with $M > M_{\text{up}}$ (where M_{up} is the maximum mass for white dwarf formation) have exploded. At that time the low-velocity winds from the evolving AGB stars begin to accumulate in the core and give rise to the second stellar generation, with $Y \sim 0.40$. This can last until *there are new Type II supernova explosions from evolving binaries*, which again expel the gas from the cluster.

Mass exchange between the components of primordial binaries can push the mass-accreting component with initial mass $M < M_{\text{up}}$ to a mass $M > M_{\text{up}}$, converting it to a Type II supernova progenitor. The timing of such supernovae is set by the time it takes the primary with mass M_1 to reach the AGB. They can continue until mass exchange is no longer capable of pushing the accreting star above M_{up} . To place a limit on this timescale, we assume that all the primary mass—apart from its white dwarf remnant—is transferred to the secondary and that the secondary initially has a mass comparable to the primary. We obtain

$$M_1 > \frac{M_{\text{up}} + M_{\text{WD}}}{2}. \quad (2)$$

For $M_{\text{up}} = 7 M_{\odot}$ and $M_{\text{WD}} = 1 M_{\odot}$, the primary mass must be larger than $4 M_{\odot}$. While a more precise estimate of this value is needed, it is not inconsistent with our expectation that the winds will initiate a third star formation epoch when $M_{\text{AGB}} \sim 4.5 M_{\odot}$.

The hypothesis of late Type II supernova explosions may be an important ingredient in the GC evolution. In particular, M_{up} decreases for smaller metallicities: this may explain the smaller degree of chemical abundance variations in the lowest metallicity clusters, as the late Type II supernova from binary evolution will last in the cluster for a longer time (see eq. [2]), preventing star formation for such a long time that the conditions for producing a new stellar generation, in addition to the first burst, become more difficult.

5. DISCUSSION AND CONCLUSIONS

We have presented *HST* observations of the MS of the GC NGC 2808, which provide important new evidence concerning the early evolution of GCs. Of the MS stars, 15%–20% are bluer by $\delta(V - I) \sim -0.1$ than the bulk of the MS stars (80%–85%), whose colors follow a normal distribution with standard deviation consistent with the observational errors. The blue MS objects are most simply interpreted as a group of stars substantially coeval with the other cluster stars ($\Delta t \leq 50$ Myr) but with a helium abundance of $Y \simeq 0.40$. The two most obvious anomalies of the CM diagram of NGC 2808, namely, (1) the blue MS stars and (2) the very peculiar morphology of the HB, can be simultaneously reproduced by means of the variations of the single parameter Y .

This is not the first time it has been proposed that the helium content plays a role in the MS morphology. In ω Cen, the presence of a high-helium MS has been suggested (Bedin et al. 2004; Norris 2004) as one of the possible components needed to explain the complexity of this cluster, in which multiple TOs and RGBs have been detected (see Lee et al. 1999; Pancino et al. 2000; Ferraro et al. 2004; Bedin et al. 2004; Sollima et al. 2005, and references therein).

Recently, on the basis of the magnitude difference between the TO and the red giant bump, Caloi & D'Antona (2005) proposed a difference in the global helium content of M3 and M13, showing that such interpretation provides subtle and consistent differences in the TO morphologies. The higher helium in M13 can also account for its much bluer HB.

In NGC 2808, *the evidence for a high-helium population is much more compelling than in the other quoted cases*, as the cluster could have been considered a standard “simple stellar population,” having no metallicity spread (in terms of Fe and alpha elements, see Carretta et al. [2004] and references therein),⁷ contrary to the ω Cen case. In addition, the evidence is based on relative photometric measurements of the MS and not on a comparison of different clusters' CM diagrams, as in the case of M3 and M13.

The case for cluster self-enrichment from the ejecta of massive AGB stars is strengthened by the present discovery of a high-helium population (see also Carretta et al. 2003, 2004 and references therein for other possible signatures of early self-enrichment). The enrichment in helium is one of the more robust predictions in the computation of the stellar yields from AGB stars and is much less model dependent than the processing of the CNO and of the other proton-capture elements (Ventura et al. 2001). The precise abundance of the high-helium population depends on the color- T_{eff} transformations, and we urge the computation of model atmospheres with the cluster chemical abundances and taking into account helium enhancement.

While it is common knowledge that helium abundance affects many phases of GC evolution, it has generally been ignored in the studies of globular clusters in recent decades. Our results suggest that helium abundance may play a major role in determining differences in the populations of different clusters *and* within the population of a given cluster; hence, its possible influence should not be neglected.

We propose a possible scenario that simultaneously accounts for the anomalous MS and HB observed in the CMD of NGC 2808 in terms of variations of helium abundance. Our scenario suggests *three main stages of star formation* in NGC 2808, all of them globally lasting not more than 200 Myr: a *first* burst at the big bang abundance, $Y = 0.24$; a *second* one from the gas of the most massive AGBs at $Y \simeq 0.40$; and a *third* one from less massive AGBs, with Y from $Y \sim 0.29$ down to ~ 0.26 and a Y distribution peaked at $Y \simeq 0.27$. In this framework, the late binary Type II supernova explosions may play a major role in producing the postulated discontinuity in helium abundance between $Y \sim 0.40$ and ~ 0.29 .

We must be careful not to overinterpret our results. The existence of the high-helium ($Y \sim 0.40$) population seems robust, since it is based both on the MS spread and HB morphology. The intermediate-helium population is inferred only from the HB morphology. Some support is given by the fact that the reddest stars of the blue HB are slightly more luminous than the red clump stars. The different luminosities result naturally from the slight difference in the Y of the red clump and the red side of the blue HB (D'Antona & Caloi 2004). However, as our discussion also shows, the interpretation of HB morphology is always intertwined with the question of mass loss. Hence, independent observational evidence is required to check the actual existence of this intermediate- Y population. In this respect, we consider the cluster RR Lyrae variables. Recently, their number has been raised from 2 to 18 (Corwin et al. 2004). The mean periods of RRab and RRc pulsators are ~ 0.563 and 0.30 days, respectively; the ratio N_c/N_{ab} is about 0.44. The latter value would favor a classification of RR Lyrae objects as Oosterhoff type II, while the

⁷ In addition to the 20 stars examined in Carretta et al. (2004), E. Carretta et al. (2005, private communication) have now reduced 123 high-resolution spectra of red giants in NGC 2808: according to this new analysis, the maximum metallicity spread allowed by the data amounts to a few hundredths of dex (± 0.03).

mean periods indicate an Oosterhoff type I (OoI). The mean periods suggest for these variables a luminosity close to that in other OoI GCs such as M3 and M5. Since for the stellar population in the latter clusters (at least for its bulk) there is no indication of a larger than cosmological helium abundance, the RR Lyrae periods observed in NGC 2808 may be considered an indirect hint for a close to normal value of Y . This is not a surprise, as the RR Lyrae objects could be the bluest extension of the red clump population, which has a normal Y , but unfortunately, does not provide us any further support for the existence of the intermediate- Y population.

Our observations suggest a possible observational strategy to search for the effects of early nucleosynthesis in GCs. Why has a clear MS bimodality been discovered so far only in this cluster and in ω Cen? First, the signal of an extreme helium-rich population is very weak and requires deep and accurate photometry in uncrowded regions of massive globulars. Only by means of these observations we may reveal the same signature observed in NGC 2808, e.g., an anomalous blue population in the sloped part of the MS with no counterpart in the TO region. Obvious candidates may be clusters with multimodal HB morphology such as NGC 1851, NGC 6441, and NGC 6388, but the first cluster has no published *HST* photometry, and the test may not be feasible for the latter two clusters because they are significantly affected by differential reddening, which may smear out as subtle a signal as the one offered in evidence in the present analysis (Rich et al. 1997). In any case, the spatial resolution and photometric accuracy required to identify a minor component of anomalous MS stars within a globular cluster are quite challenging, and it may turn out that the interesting clusters accessible with this technique are very few. The individual history of each cluster will also affect the consistency of the extreme population: if it is as low as, say, 10% of the total, it can easily pass unnoticed. Note that even *HST* MS photometry is useless to discriminate stars with helium contents from $Y = 0.24$ to 0.28 , although such a small spread corresponds to large CNO and sodium anomalies (see, e.g., the models by Ventura et al. 2002).

Finally, we want to draw the readers' attention to a few interesting facts that may be intimately related with the above results

and discussion. First, it is worth noting that the extreme blue HB becomes fainter and fainter with increasing helium abundance and the ZAHB loci at various Y -values intersect each other (see Fig. 5). As a consequence the group of HB stars fainter than the "normal" ZAHB detected, e.g., in ω Cen and in NGC 2808 with UV observations (D'Cruz et al. 2000; Brown et al. 2001) could perhaps be interpreted as belonging to a subpopulation having a helium abundance higher than those populating the "normal" ZAHB, in agreement with the suggestions put forward to explain the other main branches (Norris 2004).

Second, Fusi Pecci et al. (1993) pointed out a correlation between the extension of blue HB tails and the integrated absolute magnitude of globular clusters, which is particularly evident when the sample is restricted to clusters with intermediate metallicity ($-1.9 < [\text{Fe}/\text{H}] < -1.2$), in which, as discussed in that paper, the sensitivity to any second parameter effect is more visible. If self-enrichment (and multiple bursts of star formation) can increase the helium abundance of subsamples of stars, it seems quite natural to imagine that more massive (and/or more concentrated) clusters would be more effective in keeping the helium-enriched ejecta of AGB stars and, in turn, more efficient in producing stars populating the bluest part of the HB.

Third, Burstein et al. (2004) found that there is a marked difference in nitrogen abundance for the stars in the old M31 GCs relative to those in the oldest Galactic GCs. As they noted, the M31 GCs for which very strong NH absorption has been detected have absolute luminosities ranging from $M_V = -11$ to -9 , i.e., are very bright and massive. Therefore, it can be conceived that this peculiar enhancement is indicative of a corresponding higher helium abundance, as, within the framework described here, nitrogen and helium enhancements could result from the self-pollution occurring during the first stages of cluster life.

In conclusion, while we are *not* claiming that the whole variety of not fully understood phenomena encountered in Galactic globular clusters can be explained in terms of variations in helium abundance, the case of NGC 2808 strongly indicates that such variations do occur in real clusters and early AGB nucleosynthesis may play a significant role in the evolution of at least some of them.

REFERENCES

- Bedin, L. R., Piotto, G., Anderson, J., Cassisi, S., King, I. R., Momany, Y., & Carraro, G. 2004, *ApJ*, 605, L125
- Bedin, L. R., Piotto, G., Zoccali, M., Stetson, P. B., Saviane, I., Cassisi, S., & Bono, G. 2000, *A&A*, 363, 159
- Bellazzini, M., Fusi Pecci, F., Messineo, M., Monaco, L., & Rood, R. T. 2002, *AJ*, 123, 1509
- Bellazzini, M., Ibata, R., Monaco, L., Martin, N., Irwin, M. J., & Lewis, G. F. 2004, *MNRAS*, 354, 1263
- Bertin, E., & Arnouts, S. 1996, *A&AS*, 117, 393
- Bessell, M. S., Castelli, F., & Plez, B. 1998, *A&A*, 333, 231
- Brown, T. M., Sweigart, A. V., Lanz, T., Landsman, W. B., & Hubeny, I. 2001, *ApJ*, 562, 368
- Burstein, D., et al. 2004, *ApJ*, 614, 158
- Caloi, V., & D'Antona, F. 2005, *A&A*, 435, 987
- Carretta, E., Bragaglia, A., & Cacciari, C. 2004, *ApJ*, 610, L25
- Carretta, E., Bragaglia, A., Cacciari, C., & Rossetti, E. 2003, *A&A*, 410, 143
- Castellani M., & Castellani V. 1993, *ApJ*, 407, 649
- Catelan, M., & de Freitas Pacheco, J. A. 1995, *A&A*, 297, 345
- Corwin, T. M., Catelan, M., Borissova, J., & Smith, H. A. 2004, *A&A*, 421, 667
- Cottrell, P. L., & Da Costa, G. S. 1981, *ApJ*, 245, L79
- D'Antona, F. 2003, *Mem. Soc. Astron. Italiana Suppl.*, 3, 64
- D'Antona, F., & Caloi, V. 2004, *ApJ*, 611, 871
- D'Antona, F., Caloi, V., Montalbán, J., Ventura, P., & Gratton, R. 2002, *A&A*, 395, 69
- D'Antona, F., Gratton, R., & Chieffi, A. 1983, *Mem. Soc. Astron. Italiana*, 54, 173
- D'Cruz, N. L., Dorman, B., Rood, R. T., & O'Connell, R. W. 1996, *ApJ*, 466, 359
- D'Cruz, N. L., et al. 2000, *ApJ*, 530, 352
- Denissenkov, P. A., & Herwig, F. 2003, *ApJ*, 590, L99
- Dolphin, A. E. 2000, *PASP*, 112, 1383
- Fenner, Y., Campbell, S., Karakas, A. I., Lattanzio, J. C., & Gibson, B. K. 2004, *MNRAS*, 353, 789
- Ferraro, F. R., Messineo, M., Fusi Pecci, F., De Palo, M. A., Straniero, O., Chieffi, A., & Limongi, M., 1999, *AJ*, 118, 1738
- Ferraro, F. R., et al. 2004, *ApJ*, 603, L81
- Fusi Pecci, F., & Bellazzini, M. 1997, in *The Third Conference on Faint Blue Stars*, ed. A. G. D. Phillips, J. Liebert, R. Saffer, & D. S. Hayes (Schenectady: L. Davis), 255
- Fusi Pecci, F., Ferraro, F.-R., Bellazzini, M., Djorgovski, S. G., Piotto, G., & Buonanno, R. 1993, *AJ*, 105, 1145
- Gratton, R. G., Sneden, C., & Carretta, E. 2004, *ARA&A*, 42, 385
- Gratton, R. G., et al. 2001, *A&A*, 369, 87
- Harris, W. E. 1996, *AJ*, 112, 1487
- Lattanzio, J., Karakas, A., Campbell, S., Elliott, L., & Chieffi, A. 2004, *Mem. Soc. Astron. Italiana*, 75, 322
- Lee, Y.-W., et al., 1999, *Nature*, 402, 55
- . 2005, *ApJ*, 621, L57
- Martin, N., Ibata, R., Bellazzini, M., Irwin, M. J., Lewis, G. F., & Dehnen, W. 2004, *MNRAS*, 348, 12
- Martinez-Delgado, D., Butler, D. J., Rix, H.-W., Franco, Y. I., & Penarrubia, J. 2005, *ApJ*, in press (astro-ph/0410611)
- Moehler S., Sweigart A. V., Landsman W. B., Hammer N. J., & Dreizler S. 2004, *A&A*, 415, 313
- Norris, J. E. 2004, *ApJ*, 612, L25

- Pancino, E., Ferraro, F. R., Bellazzini, M., Piotto, G., & Zoccali, M. 2000, *ApJ*, 534, L83
- Rich, M. R., et al. 1997, *ApJ*, 484, L25
- Rogers, F. J. 2001, *Contrib. Plasma Phys.*, 41, 179
- Rood, R. T. 1973, *ApJ*, 184, 815
- Rood, R. T., & Crocker, D. A. 1989, in *IAU Colloq. 11, The Use of Pulsating Stars in Fundamental Problems of Astronomy* (Cambridge: Cambridge Univ. Press), 103
- Saumon, D., Chabrier, G., & van Horn, H. M. 1995, *ApJS*, 99, 713
- Schechter, P., Mateo, M., & Saha, A. 1993, *PASP*, 105, 1342
- Snedden, C. 1999, *Ap&SS*, 265, 145
- . 2000, in *The Galactic Halo: From Globular Clusters to Field Stars*, ed. A. Noels, P. Magain, D. Caro, E. Jehin, G. Parmentier, & A. Thoul (Liège: Inst. Astrophys. Géophys.), 159
- Sollima, A., Ferraro, F. R., Pancino, E., & Bellazzini, M. 2005, *MNRAS*, 357, 265
- Stolzmann, W., & Bloeker, T. 1996, *A&A*, 314, 1024
- . 2000, *A&A*, 361, 1152
- Sweigart, A. V. 1997, *Third Conference on Faint Blue Stars*, ed. A. G. D. Philip, J. Liebert, R. Saffer, & D. S. Hayes (Schenectady: L. Davis), 3
- Trager, S. C., Djorgovski, S. G., & King, I. R. 1993, in *ASP Conf. Ser. 50, Structure and Dynamics of Globular Clusters*, ed. S. Djorgovski & G. Meylan (San Francisco: ASP), 347
- Ventura, P., & D'Antona, F. 2005a, *A&A*, 431, 279
- . 2005b, *A&A*, in press (astro-ph/0505221)
- Ventura, P., D'Antona, F., & Mazzitelli, I. 2002, *A&A*, 393, 215
- Ventura, P., D'Antona, F., Mazzitelli, I., & Gratton, R. 2001, *ApJ*, 550, L65
- Ventura, P., Mazzitelli, I., & D'Antona, F. 2004, *Mem. Soc. Astron. Italiana*, 75, 335